Available online at www.sciencedirect.com

ScienceDirect

Geochimica et Cosmochimica Acta 71 (2007) 745–759

Geochimica

www.elsevier.com/locate/gca

Isotope systematics of Li, Sr, Nd, and volatiles in Indian Ocean MORBs of the Rodrigues Triple Junction: Constraints on the origin of the DUPAL anomaly

Yoshiro Nishio [a,*], Shun'ichi Nakai [b], Teruaki Ishii [c], Yuji Sano [c]

[a] *Kochi Institute for Core Sample Research, Japan Agency for Marine-Earth Science and Technology (JAMSTEC), Monobe B200, Nankoku, Kochi 783-8502, Japan*

[b] *Earthquake Research Institute, University of Tokyo, Yayoi 1-1-1, Bunkyo, Tokyo 113-0032, Japan*

[c] *Ocean Research Institute, University of Tokyo, Minamidai 1-15-1, Nakano, Tokyo 164-8639, Japan*

Received 2 May 2006; accepted in revised form 6 October 2006

Abstract

The DUPAL anomaly, a radiogenic isotope anomaly discovered in the Indian Ocean mantle, has been interpreted as due to a large-scale mantle heterogeneity. To provide new constraints on the DUPAL origin, we analyzed isotope ratios of Li, Sr, and Nd in fresh N-MORB glasses recovered from the Rodrigues Triple Junction in the Indian Ocean, and from the North Atlantic. The Li isotopic compositions of the Indian Ocean DUPAL N-MORBs were comparable to those of the North Atlantic non-DUPAL N-MORBs. The source of the DUPAL signature in Indian Ocean MORBs and the E-MORB-type enriched mantle source have quite different Li isotopic compositions. The $^{143}Nd/^{144}Nd$ values of both sources are significantly lower than those of the North Atlantic N-MORBs. The δ^7Li values of most oceanic island basalts with similar low $^{143}Nd/^{144}Nd$ signatures are also higher than those of the North Atlantic N-MORBs, except for several Koolau lavas. The Li isotope results support the recent proposal that significant amounts of recycled lower continental crust might produce the radiogenic isotope signatures of the Indian Ocean DUPAL source.

1. Introduction

Indian Ocean MORBs typically have higher $^{87}Sr/^{86}Sr$ and lower $^{206}Pb/^{204}Pb$ and $^{143}Nd/^{144}Nd$ than North Atlantic (N-Atlantic) and East Pacific (E-Pacific) MORBs, and these isotopic characteristics of Indian Ocean MORBs are representative of the DUPAL anomaly (e.g., Dupre et al., 1981; Hart, 1984). Previous studies using Sr, Nd, and Pb isotope tracers (e.g., Rehkamper and Hofmann, 1997 and references therein) considered the DUPAL signature to result from contamination by recycled continental lithosphere, either old subcontinental lithosphere or sediments associated with subducting oceanic crust. Alternatively, the lower continental crust (LCC) may be the source of the DUPAL signature of Indian Ocean MORBs, as suggested by new Hf and Os isotope results (Escrig et al., 2004; Hanan et al., 2004).

Lithium is an alkali metal trace element that is moderately incompatible during mantle melting (e.g., Brenan et al., 1998). It is a fluid-mobile element, which is a univalent cation (Li^+) in solution, and it provides information different from that provided by well-known radiogenic isotope tracers such as Sr, Nd, and Pb. Lithium has two stable isotopes, ^7Li and ^6Li, with abundances of 92.5% and 7.5%, respectively. The large difference in mass between these two isotopes leads to high levels of isotopic fractionation during near-surface processes. Thus, Li abundance and isotope ratios have been used as tracers for near-surface subducted material in the mantle. Subducted components ($\delta^7Li < +14‰$) such as altered oceanic crust (Chan et al., 2002) and marine sediments (Chan and Kastner, 2000) have a heavier Li isotopic signature than the mantle ($\delta^7Li = +3‰$, this study), where $\delta^7Li = [[^7Li/^6Li]_{sample}/$

---

[*] Corresponding author. Fax: +81 46 867 9315.
E-mail address: nishio@jamstec.go.jp (Y. Nishio).

0016-7037/$ - see front matter © 2006 Elsevier Inc. All rights reserved.
doi:10.1016/j.gca.2006.10.004

$[^7Li/^6Li]_{L\text{-}SVEC\ standard} - 1] \times 1000$. During subduction, substantial Li isotopic fractionation between dehydrated fluid and the residual slab occurs: the δ^7Li value of Li in dehydrated fluid is expected to be higher than that of residual slab Li (Zack et al., 2003). Zack et al. (2003) based their model on dramatically low δ^7Li values (−11‰ to +5‰) in eclogites from Trescolmen, Switzerland.

As the Li isotope ratio is not affected by time, or by parent–daughter fractionation, it can provide information about the DUPAL anomaly to complement that from radiogenic isotope tracers. We analyzed Li isotope ratios of fresh zero-age Indian Ocean and N-Atlantic MORBs. Reports of Li isotope data from fresh MORBs (Chan et al., 1992; Moriguti and Nakamura, 1998; Tomascak and Langmuir, 1999; Nishio et al., 2002; Elliott et al., 2003) do not always adequately describe the freshness and chemical composition of the MORBs. The freshness of MORB samples is crucial because their δ^7Li values tend to increase because of the uptake over time of heavy Li isotopes from seawater (Chan et al., 1992, 2002). Knowledge of the chemical composition of analyzed MORBs is also crucial to assess the DUPAL signature, because the δ^7Li values of MORBs increase with $^{87}Sr/^{86}Sr$ and La/Sm ratios, and decrease with $^{143}Nd/^{144}Nd$ ratios (Elliott et al., 2003, 2004).

2. Samples

All samples used in this study were from fresh glass portions of the chilled margins of deep-sea lavas (water depth, 2500–4100 m). Abundant volatiles are preserved in quenched glass because it forms under high hydraulic pressure and cools rapidly; therefore, quenched glass portions of lavas are commonly used for studies of mantle volatiles (e.g., Marty and Ozima, 1986; Nishio et al., 1998; Nishio et al., 1999). Marginal glasses are also ideal samples of abyssal lava for the study of elements sensitive to seawater alteration (e.g., Sr and Li), because fresh marginal glass is the least altered portion.

Samples were collected from the Indian Ridge near the Rodrigues Triple Junction (RTJ) (25.6°S, 70.0°E). Sample locations and a bathymetric map of the RTJ area have previously been published (Nishio et al., 1999). At the RTJ, three ridges with different spreading rates meet: the Central Indian Ridge (CIR), the Southeast Indian Ridge (SEIR), and the Southwest Indian Ridge (SWIR). The samples analyzed in this study were dredged at stations KH93-3-DR1 (CIR adjacent to RTJ), KH93-3-DR3 (CIR adjacent to RTJ), KH93-3-DR6 (SEIR adjacent to RTJ), KH93-3-DR9 (immediate area of RTJ), and KH93-3-DR25 (immediate area of RTJ) during the KH93-3 cruise of the R/V *Hakuho Maru* (Ocean Research Institute, University of Tokyo). We also analyzed samples of N-Atlantic mid-oceanic ridge lava glasses: 224-R-01 (26.1°N, 44.8°W), CH98-DR11 (30.7°N, 41.8°W), and CH31-DR11 (36.8°N, 33.3°W). Sample 224-R-01 was recovered from the Trans-Atlantic Geotraverse (TAG) hydrothermal mound area (Rona et al., 1986) by the submersible *Shinkai 6500*, JAMSTEC (Fujioka et al., 1995). Both CH98-DR11 (Bougault and Treuil, 1980) and CH31-DR11 (Bougault and Hekinian, 1974) were dredged samples.

We also analyzed Loihi glasses to identify δ^7Li values of a high $^3He/^4He$ mantle source. The Loihi Seamount, south of the Big Island of Hawaii, is the youngest expression of hotspot volcanism in the Hawaiian–Emperor chain (Moore et al., 1982). The Loihi Seamount is mainly covered by talus, and there is a ridge in its south rift zone (Valbracht et al., 1997), where samples KH85-4-DE55-1 (along the ridge) and KH85-4-DE54-025 (east slope of the ridge) were dredged during the KH85-4 cruise of the R/V *Hakuho Maru*.

Except for the TAG sample and the two Loihi samples, major elemental compositions and volatile data (C, N, He, and Ar) have been reported previously (Nishio et al., 1998, 1999; Sano et al., 1998). Noble gas data, including Ne, Kr, and Xe, of several studied samples are also available (Hiyagon et al., 1992; Kumagai and Kaneoka, 2003, 2005). Kumagai and Kaneoka (2003) reported the relationship between textures and the noble gas signatures of the studied RTJ Indian Ridge samples.

3. Analytical procedure

Fresh glass fragments, without oxidation haloes, from the chilled margins of deep-sea lava blocks were handpicked after repeated crushing. Collected glass fragments were washed ultrasonically in a 5% HNO_3 solution (15 min) and then cleaned consecutively in distilled water, ethanol, and acetone (15 min each). A weak HNO_3 solution was used to avoid Li isotopic fractionation during washing (Nishio et al., 2004, 2005). The δ^7Li values of standard samples (SRM 612 50 μg g^{-1} Trace Element Glass standard) with and without leaching in 5% HNO_3 solution (+31.7‰ and +32.4‰, respectively) agreed within analytical errors and suggest that the observed Li isotopic ratios were not significantly affected by 15 min of leaching with HNO_3 solution.

The isotopic and elemental compositions of CO_2, N_2, He, and Ar in vesicle gas from marginal glasses were first analyzed using the vacuum crushing technique. The detailed procedures for volatile analysis are described by Takahata et al. (1998) and Nishio et al. (1999). The crushed residue was subsequently finely ground in an agate mortar. After digestion of the powdered samples (0.05 g) by concentrated HF and $HClO_4$, the resulting solution was divided into two aliquots: one for measurement of Li–Sr–Nd isotopic ratios and the other for measurement of trace elemental abundances. After column separation using cation exchange resin AG 50W-X8 (Bio-Rad Laboratories Inc.) and Ln resin (Eichrom Technologies Inc.), Li, Sr, and Nd isotopic ratios were determined in solutions with about 100 ng g^{-1} Li, 100 ng g^{-1} Sr, and 50 ng g^{-1} Nd, respectively, using a MC-ICP-MS Isoprobe (GV Instruments Inc, previously Micromass). Samples were introduced into the spectrometer via an Aridus desolvating unit (Cetac Technologies). A T1H nebulizer (Cetac Technologies) was used for Li isotope measurements, whereas a micromist nebulizer

(Glass Expansion Pty Ltd) was used for Sr and Nd isotope measurements. Procedural blanks for Li, Sr, and Nd isotope analyses were less than 10 pg, 50 pg, and 10 pg, respectively. The Li standard solution (NIST L-SVEC) was measured before and after sample analyses to correct for instrumental mass bias in the Li isotope measurements. The $^{87}Sr/^{86}Sr$ and $^{143}Nd/^{144}Nd$ data were normalized to $^{87}Sr/^{86}Sr = 0.710258$ for SRM987, and $^{143}Nd/^{144}Nd = 0.5121067$ for JNdi-1. The δ^7Li, $^{87}Sr/^{86}Sr$, and $^{143}Nd/^{144}Nd$ values we obtained for standard volcanic rocks agreed well (within statistical errors) with previously published data ($\delta^7Li = \pm 0.83‰$; $^{87}Sr/^{86}Sr = \pm 0.00006$; $^{143}Nd/^{144}Nd = \pm 0.000027$, 2SD) (Nishio and Nakai, 2002; Nishio et al., 2004). Details of the Li–Sr–Nd isotopic analytical protocols we used have been documented previously (Nishio and Nakai, 2002; Nishio et al., 2004, 2005). Li abundance was determined by MC-ICP-MS after column separation (Nishio and Nakai, 2002). Analytical errors for Li abundances were better than 12% (2RSD), as estimated from the reproducibility of standard rocks (Nishio and Nakai, 2002). Other trace elemental abundances were determined with a quadrupole ICP-MS (PQ3, Thermo Elemental), without purification, and with the matrix effect corrected by using internal standards of indium and rhenium. The major elemental abundances of lava glass samples (other than sample KH85-4-DE54-025, which was too small) were determined by XRF (PW1480, Philips Co.) using portions of powdered samples (0.4 g) (Yoshida and Takahashi, 1997). Sample KH85-4-DE54-025 was analyzed with a broad beam (15 μm diameter) EPMA (JXA-8900RL, JEOL Ltd).

4. Results

Isotopic compositions of Li, Sr, Nd, He, Ar, C, and N in the lava samples are listed in Table 1, together with other useful indices. All trace element analyses are provided in Appendix 1, together with reference rock data and reproducibilities. All analyses for major elements and volatiles of the TAG sample and two Loihi samples are listed in Appendix 2; those of the other samples studied have been reported previously (Nishio et al., 1998; Sano et al., 1998; Nishio et al., 1999).

The SiO_2 and $Na_2O + K_2O$ concentrations and the chondrite-normalized $(La/Sm)_n$ values indicate that all the mid-oceanic ridge samples we studied were N-MORBs (Table 1). Michard et al. (1986) reported that all of the Indian Ocean MORBs that they recovered from the RTJ area were N-MORBs (Fig. 1a and b). The $^3He/^4He$ (R/R_A) and $^{40}Ar/^{36}Ar$ values of the studied MORBs varied from 8.0 to 9.0 and from 515 to 19 000, respectively (Table 1). Values of $^3He/^4He$ of around 8 R/R_A (e.g., Hilton et al., 1993) and those of high $^{40}Ar/^{36}Ar$ (Burnard et al., 1997) are characteristic of fresh MORB glasses. The δ^7Li values of N-MORB glasses obtained in this study (+2.4‰ to +4.1‰) cover a narrower range than those of previous studies (+1.5‰ to +6.5‰) (Chan et al., 1992; Moriguti and Nakamura, 1998; Tomascak and Langmuir, 1999; Elliott et al., 2003). The $^{87}Sr/^{86}Sr$ and $^{143}Nd/^{144}Nd$ ratios of the RTJ N-MORBs are, respectively, higher and lower than those of the N-Atlantic N-MORBs (Fig. 1c). The $^{87}Sr/^{86}Sr$ and $^{143}Nd/^{144}Nd$ values observed in this study (Fig. 1a–c) agree well with previous results for RTJ N-MORBs recovered from the same area (25.2–25.8°S, 69.9–70.2°E) (Michard et al., 1986; Price et al., 1986). In contrast to Sr–Nd isotopic data, no significant difference in Li isotopic composition was observed between RTJ N-MORBs (+2.4‰ to +4.1‰) and N-Atlantic N-MORBs (+2.7‰ to +3.4‰) (Table 1).

The $^3He/^4He$ ratios (25 R/R_A and 30 R/R_A) and $^{40}Ar/^{36}Ar$ ratios (490 and 669) of the studied Loihi basalt glasses were, respectively, higher and lower than the MORB values (Table 1). The $(La/Sm)_n$ values for the Loihi samples ranged from 1.6 to 1.8, and were significantly higher than those of the N-MORBs (Table 1). The $^{87}Sr/^{86}Sr$ (0.7036) and $^{143}Nd/^{144}Nd$ (0.51295–0.51296) values of the Loihi samples were, respectively, higher and lower than the obtained N-MORB values (Table 1). The δ^7Li values of the Loihi glasses (+4.1‰ and +5.5‰) were higher than the average N-MORB value (+3.2 ± 1.3‰, 2SD) obtained in this study (Table 1).

5. Discussion

5.1. Seawater alteration

The δ^7Li values observed in the N-MORBs fell within a narrow range from +2.4‰ to +4.1‰, while the $^{40}Ar/^{36}Ar$ ratios varied greatly from 515 to 19 000 (Fig. 2). Thus, the results of this study showed that pristine δ^7Li values can be observed in MORB glasses with $^{40}Ar/^{36}Ar$ ratios higher than 515. Using Li isotopic results from altered MORBs, Chan et al. (1992) estimated the alteration δ^7Li end-member value to be +14‰. Using this value, the expected Li–Ar isotope shift of N-MORBs as a result of progressive seawater alteration is shown in Fig. 2.

Potassium/rubidium ratios have been proposed as an index of progressive seawater alteration of abyssal basalts (Hart, 1969; Verma, 1992). The δ^7Li values observed in the N-MORBs fell within a narrow range from +2.4‰ to +4.1‰, while the K/Rb ratios varied from 350 to 740. Accordingly, our results indicated that pristine δ^7Li values can be observed in MORBs with K/Rb ratios between 350 and 740.

5.2. The DUPAL signature of the RTJ N-MORBs

5.2.1. Sr, Nd, and Li isotopes

The expected Sr–Nd isotope shifts of N-Atlantic MORBs as a result of progressive seawater alteration were estimated from the results of binary mixing between N-Atlantic MORBs and seawater (Fig. 1c) (end-member values used for the mixing calculation are in Appendix 3). This plot demonstrates that the Sr and Nd isotopic differences between Indian Ocean and N-Atlantic MORBs cannot be explained by seawater alteration.

Table 1
Li–Sr–Nd–He–Ar–C–N isotopic compositions and key indices of marginal glasses of pillow lavas from the RTJ Indian Ocean and North Atlantic mid-oceanic ridges and the south rift zone of Loihi Seamount, Hawaii

Sample	Indian Ridges (Triple Junction area)					North Atlantic Ridge			Seamount (Hawaii)		[Uncertainly][a]
	KH93-3-DR3-A1	KH93-3-DR1-F1	KH93-3-DR9-G1	KH93-3-DR25-A1	KH93-3-DR6-A1	224-R-01	CH98-DR11	CH31-DR11	KH85-4-DE54-025	KH85-4-DE55-1	
Site[b]	CIR	CIR	RTJ	RTJ	SEIR	NAR (TAG)	NAR	NAR	Loihi (east slope of S. rift)	Loihi (on S. rift)	
Latitude	25.23°S	25.37°S	25.50°S	25.58°S	25.80°S	26.14°N	30.68°N	36.83°N	18.82°N	18.80°N	
Longitude	69.92°E	70.03°E	70.07°E	70.07°E	70.22°E	44.83°W	41.82°W	32.25°W	155.20°W	155.20°W	
Depth (m)	4090	4030	4080	4270	3640	3646	3600	2480	3260	3180	
δ^7Li (‰)	+4.1	+2.5	+4.0	+2.4	+3.0	+3.4	+3.2	+2.7	+5.5	+4.1	[±0.83‰, 2SD]
^{87}Sr/^{86}Sr	0.70309	0.70307	0.70310	0.70313	0.70318	0.70255	0.70254	0.70281	0.70363	0.70356	[±0.00006, 2SD]
^{143}Nd/^{144}Nd	0.513043	0.513040	0.513087	0.513079	0.513049	0.513187	0.513212	0.513186	0.512962	0.512953	[±0.000027, 2SD]
^{3}He/^{4}He (R/R$_A$)	8.47[d]	8.13[d]	7.96[d]	8.42[d]	8.55[d]	8.46	8.97[d]	8.64[d]	30.4	25.3	[±10%, 2RSD]
^{40}Ar/^{36}Ar	3150[e]	515[d]	11,300[d]	17,000[e]	4950[e]	6760	19,000[e]	5190[e]	490	669	
[2SD][c]	±130	±15	±1300	±4000	±320	±580	±12,000	±890	±13	±16	
δ^{13}C (‰) of CO$_2$	−2.59[d]	−2.99[d]	−5.58[d]	−3.12[d]	−3.95[d]	−2.77	−3.10[d]	−5.72[d]	−1.36	−1.90	[±0.2‰, 2SD]
δ^{15}N (‰) of N$_2$	−1.7[e]	−2.2[d]	−1.0[d]	−2.3[e]	−2.0[e]	−3.2	−3.1[e]	−1.2[e]	+0.5	+0.4	[±1‰, 2SD]
SiO$_2$ (wt%)	49.6[d]	50.1[d]	50.4[d]	51.0[d]	49.9[d]	49.9	49.6[d]	50.2[d]	46.3	46.9	[±0.6%, 2RSD]
Na$_2$O (wt%)	2.79[d]	3.08[d]	2.92[d]	2.76[d]	3.06[d]	2.82	2.50[d]	2.53[d]	2.29	2.56	[±1.3%, 2RSD]
K$_2$O (wt%)	0.03[d]	0.15[d]	0.06[d]	0.03[d]	0.05[d]	0.08	0.03[d]	0.11[d]	0.78	0.57	[±0.8%, 2RSD]
[weight ratios][f]											
Li/Yb	2.34	2.03	2.00	2.38	2.16	1.87	1.87	1.86	2.96	3.16	[±17%, 2RSD]
Li/Y	0.263	0.226	0.225	0.244	0.240	0.205	0.213	0.215	0.260	0.277	[±14%, 2RSD]
K/Rb	558	741	545	606	483	721	402	347	646	512	[±5%, 2RSD]
(La/Sm)$_n$[g]	0.51	0.81	0.60	0.54	0.59	0.59	0.51	0.84	1.8	1.6	[±12%, 2RSD]
(La/Yb)$_n$[g]	0.60	0.91	0.62	0.63	0.68	0.70	0.54	0.89	6.5	5.6	[±14%, 2RSD]
(Sm/Yb)$_n$[g]	1.2	1.1	1.0	1.2	1.1	1.2	1.0	1.1	3.6	3.4	[±16%, 2RSD]
[mole ratios]											
^{4}He/^{40}Ar*	3.9[d]	19[d]	6.6[d]	3.7[d]	3.6[d]	13	6.8[d]	12[d]	1.3	1.4	[±14%, 2RSD]
CO$_2$/^{3}He ($\times 10^9$)	0.39[d]	0.35[d]	0.33[d]	0.20[d]	0.55[d]	0.51	1.58[d]	1.92[d]	2.54	2.17	[±37%, 2RSD]

[a] Uncertainly has been estimated by reproducibility (2SD) of repeated measurement of standard material.

[b] CIR, Central Indian Ridge; RTJ, immediate area of Rodrigues Triple Junction; SEIR, Southeast Indian Ridge; NAR, North Atlantic Ridge; TAG, Trans-Atlantic Geotraverse; S. rift, South rift zone of Loihi seamount.

[c] Internal errors that are standard deviation (2SD) of acquired ^{40}Ar/^{36}Ar data within a run of the measurement.

[d] Data have been already reported in Nishio et al. (1999).

[e] Data have been already reported in Sano et al. (1998).

[f] Full data sets of the trace elemental abundances are listed in Appendix 1.

[g] CI chondrite-normalized La/Sm, La/Yb, and Sm/Yb ratios. La, Sm, and Yb abundances of the CI chondrite are from McDonough and Sun (1995).

It is also clear that the enriched Sr and Nd isotopic signatures of the RTJ MORBs are not due to an E-MORB-type enriched mantle source, because of the similarity of the La/Sm ratios of the Indian Ocean and N-Atlantic MORBs (Fig. 1a and b). The large-scale mantle heterogeneity known as the DUPAL anomaly has been expressed by Hart (1984) in terms of Δ7/4Pb and Δ8/4Pb, and defined as the vertical deviation from the Northern Hemisphere Reference Line (NHRL). Significantly high Δ7/4Pb (+6 to +12) and Δ8/4Pb (+69 to +78) values have been observed in RTJ N-MORBs with enriched Sr and Nd isotope signatures (Michard et al., 1986; Price et al., 1986). Consequently, we also attributed the enriched Sr and Nd isotope signatures that we observed in the RTJ MORBs to DUPAL contamination of the source, not to seawater alteration and/or the presence of an E-MORB-type enriched mantle source.

In contrast to the Sr and Nd isotope results, no systematic difference was observed in δ^7Li values between the RTJ N-MORBs (+3.2 ± 1.6‰, 2SD) and the N-Atlantic N-MORBs (+3.1 ± 0.7‰, 2SD). The δ^7Li values were not shifted by isotope fractionation due to crystal-melt reactions, because no systematic difference was observed in the differentiation indices, such as SiO_2 content (Table 1). Tomascak et al. (1999) also has suggested that Li isotope fractionation at the per mil level does not occur during high-temperature processes.

5.2.2. Li/Yb ratio

Ryan and Langmuir (1987) suggested that, because of the constant Li/Yb and Li/Y ratios of MORBs, the mineral–melt partitioning behavior of Li during melting and fractional crystallization closely resembles that of Yb and Y. Thus, to separate the effects of differentiation (crystal–melt equilibrium) from other Li-additional processes, Li/Yb and Li/Y ratios have been used as indicators of excess Li-enrichment of lavas (e.g., Moriguti and Nakamura, 1998; Chan et al., 1999).

The Li/Yb values of DUPAL N-MORBs ($\Delta 7/4\text{Pb} \geqslant 2.5$; $\Delta 8/4\text{Pb} \geqslant 15$) tend to be higher than those of non-DUPAL N-MORBs ($\Delta 7/4\text{Pb} < 2.5$; $\Delta 8/4\text{Pb} < 15$) (Fig. 3a and b, Appendices 4 and 5). The Li/Yb ratios of the RTJ N-MORBs (2.00–2.38) tend to be higher than those of the N-Atlantic N-MORBs (1.86–1.87). However, no difference was observed in differentiation indices such as SiO_2 content and $(La/Sm)_n$, $(La/Yb)_n$, and $(Sm/Yb)_n$ ratios between the Indian Ocean and N-Atlantic MORBs (Table 1). Among these differentiation indices, La/Yb and Sm/Yb ratios provide information on garnet-bearing differentiation, because HREEs such as Yb and Y are more compatible in garnet than Li and LREEs such as La or Sm. Consequently, the observed difference in Li/Yb values between Indian Ocean and N-Atlantic MORBs cannot be attributed to differentiation (including garnet-bearing differentiation).

5.3. Li isotope systematics of lavas having enriched Sr–Nd isotope signatures

Elliott et al. (2003) reported that δ^7Li values of E-Pacific MORBs increased from +3.1‰ to +5.2‰ with decreasing $^{143}Nd/^{144}Nd$ ratios from 0.51325 to 0.51315. The increasing δ^7Li values observed in E-Pacific MORBs have been attributed to an E-MORB-type enriched mantle source because the δ^7Li values also correlate positively with La/Sm ratios (Elliott et al., 2003, 2004). Comparison of the Li–Nd isotope trend of MORBs from the E-Pacific (Elliott et al., 2003, 2004) with data of this study (Fig. 4a) shows that the source of the DUPAL signature in Indian Ocean MORBs and the E-MORB-type enriched mantle source have quite different δ^7Li signatures of +3‰ and >+5‰, respectively, (Elliott et al., 2003, 2004) (Fig. 4a).

Comparison of Li–Nd and Li–Sr isotopic correlations of the Loihi glasses of this study with previously reported oceanic island basalt (OIB) data (Fig. 4a and b) (Chan and Frey, 2003; Ryan and Kyle, 2004; Nishio et al., 2005) showed δ^7Li values of +4.1‰ and +5.5‰ for the two Loihi glasses with high $^3He/^4He$ ratios (>25 R/R_A). These δ^7Li values are significantly higher than those of the N-Atlantic MORBs (+3.1‰). The whole-rock δ^7Li values of many OIBs from Mangaia, Tubuai Rurutu, Tahiti, Hiva Oa, Ua Pou (Polynesia), and Marie Byrd Land (Antarctica) are also higher than the N-Atlantic N-MORB value (+3‰). In contrast, the δ^7Li values of several Koolau (Hawaii) OIBs are significantly lower than those of other OIBs with similarly enriched Sr–Nd isotopic compositions (Chan and Frey, 2003) (Fig. 4a and b).

Based on Sr, Nd, and Pb radiogenic isotopic data, four end-member geochemical reservoirs have been proposed as the source of OIBs: depleted mantle (DM), high $^{238}U/^{204}Pb$ mantle (HIMU), and two types of enriched mantle (EM1 and EM2) (e.g., Zindler and Hart, 1986). From N-Atlantic non-DUPAL N-MORB data obtained in this study, we estimated +3.1 ± 0.7‰ (2SD) as the δ^7Li value of the DM end-member component. Relative to this DM value, the higher δ^7Li values of both HIMU (+5‰ to +7‰) and EM2 (>+6‰) end-member components have been reported from Polynesian OIB data (Nishio et al., 2005).

As mentioned above, the δ^7Li values of several Koolau OIBs are lower than those of other OIBs that are related to HIMU and EM2 components (Chan and Frey, 2003). Because the low $^{206}Pb/^{204}Pb$ values (17.8–17.9) of the Koolau OIBs (Roden et al., 1994) indicate the involvement of an EM1 component in their source, together with other end-member components, Nishio et al. (2004) attributed the lower δ^7Li values of the Koolau OIBs to the EM1 end-member component. Nishio et al. (2004) further inferred a low δ^7Li value of the EM1 end-member value (>–17‰), based on the results of mantle-derived ultramafic xenoliths. However, a definitive δ^7Li value of the EM1 end-member has not been determined owing to a lack of data from EM1-dominant OIBs such as Pitcairn lavas.

Based on radiogenic isotopic signatures, the involvement of an EM1 end-member component, together with an EM2 end-member component, in the Indian Ocean DUPAL source has been proposed (e.g., Agranier et al., 2005). Thus, we inferred that the relatively low δ^7Li values of the

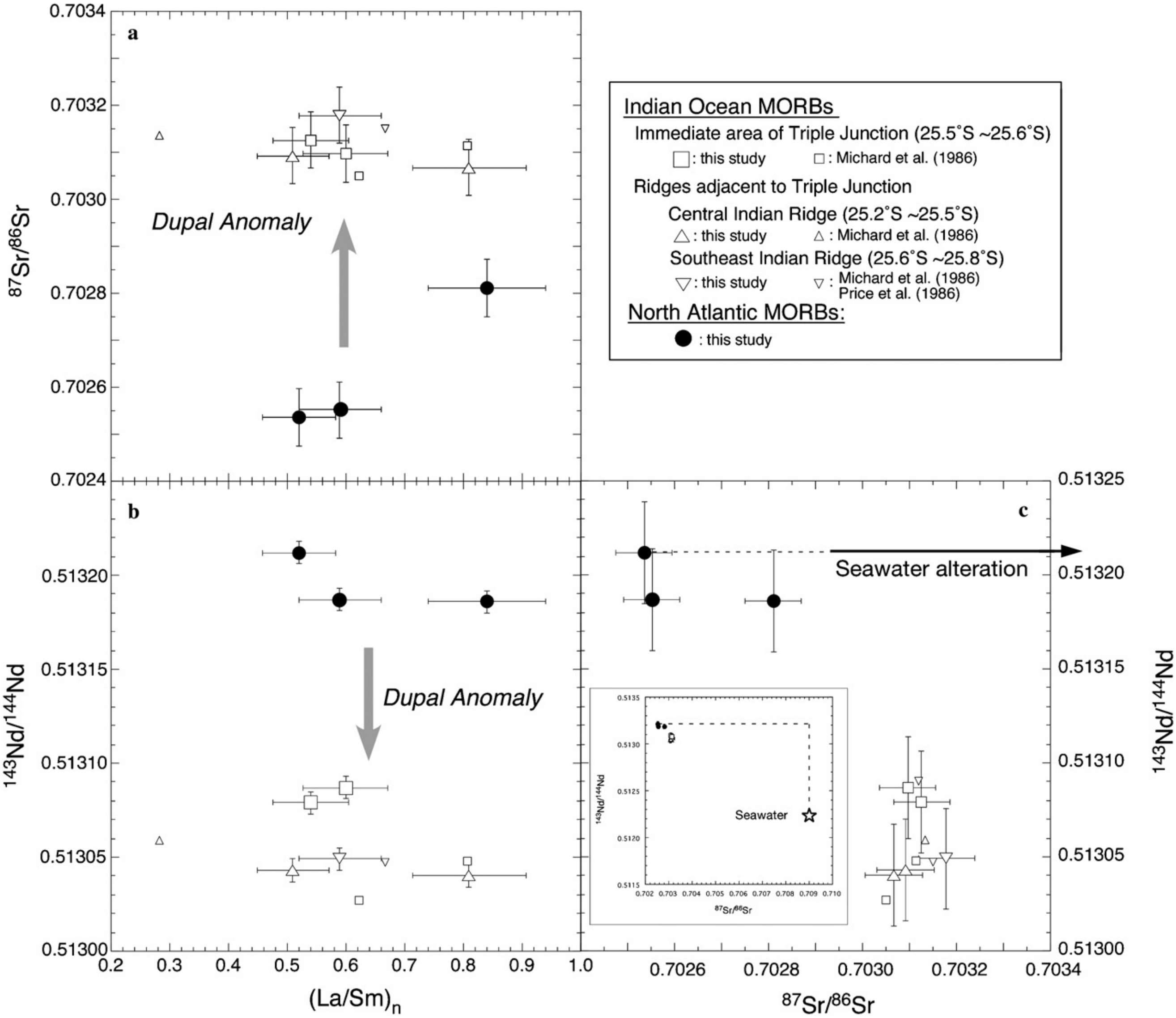

Fig. 1. Correlations of $(La/Sm)_n$ and $^{87}Sr/^{86}Sr$ (a), $(La/Sm)_n$ and $^{143}Nd/^{144}Nd$ (b), and $^{87}Sr/^{86}Sr$ and $^{143}Nd/^{144}Nd$ (c) of RTJ MORBs and N-Atlantic MORBs. Previous results for RTJ MORBs recovered from the same area as this study (25.2–25.8°S; 69.9–70.2°E) (Michard et al., 1986; Price et al., 1986) are also shown. Errors shown are listed in Table 1. The expected Sr–Nd isotope shift of the N-Atlantic N-MORBs because of progressive seawater alteration is shown as the dashed line in figure (c), and is estimated from the results of binary mixing of N-Atlantic N-MORBs and Indian Ocean deep seawater. End-member values used for the mixing calculation are listed in Appendix 3.

Indian Ocean DUPAL N-MORBs and several Koolau OIBs can be attributed to the EM1 reservoir.

5.4. Cause of the DUPAL signature in Indian Ocean MORBs

5.4.1. Recycled sediment

The $C/^3He$ ratio has been used as a sensitive indicator of recycled carbon in volcanic gases (e.g., Marty and Jambon, 1987; Sano and Marty, 1995; Sano and Williams, 1996). Kingsley and Schilling (1995) observed that $C/^3He$ values for vesicle-derived gases of the N-Atlantic MORB samples tend to increase with decreasing $^{143}Nd/^{144}Nd$ values (Fig. 5), which they interpreted to reflect a contribution from a recycled C-rich component associated with the Azores plume. Available data for less degassed MORB samples identified by $^4He/^{40}Ar^*$ values of $\leqslant 30$ are also shown in the $^{143}Nd/^{144}Nd$–$C/^3He$ ($\approx CO_2/^3He$) diagram (Fig. 5). The $^4He/^{40}Ar^*$ value is a good index of the degree of fractional degassing, because the He and Ar solubilities differ by a factor of 10. It is also likely that the $CO_2/^3He$ values of relatively less degassed MORB samples ($^4He/^{40}Ar^* \leqslant 30$) should be approximately equal to the $CO_2/^3He$ value of a pristine magma source, based on the results of calculations using the CO_2–He–Ar solubilities (Marty and Tolstikhin, 1998; Marty and Zimmermann, 1999). The $^{143}Nd/^{144}Nd$–$C/^3He$ data distribution of the Indian Ocean MORBs is quite different from those of the N-Atlantic and E-Pacific MORBs (Fig. 5). Furthermore, the $^{143}Nd/^{144}Nd$–$C/^3He$ data distribution suggests that the source of the DUPAL signature

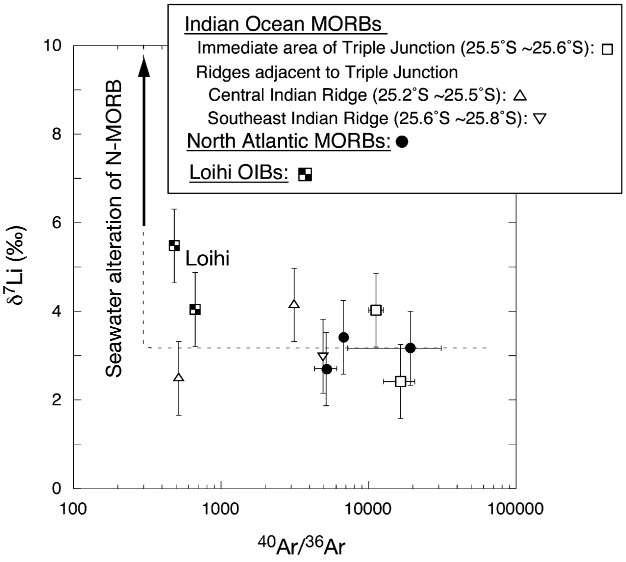

Fig. 2. Correlation of $^{40}Ar/^{36}Ar$ and δ^7Li for the N-MORBs and Loihi OIBs. Errors shown are listed in Table 1. The expected Li–Ar isotope shift of N-MORBs because of progressive seawater alteration is shown as a dashed line.

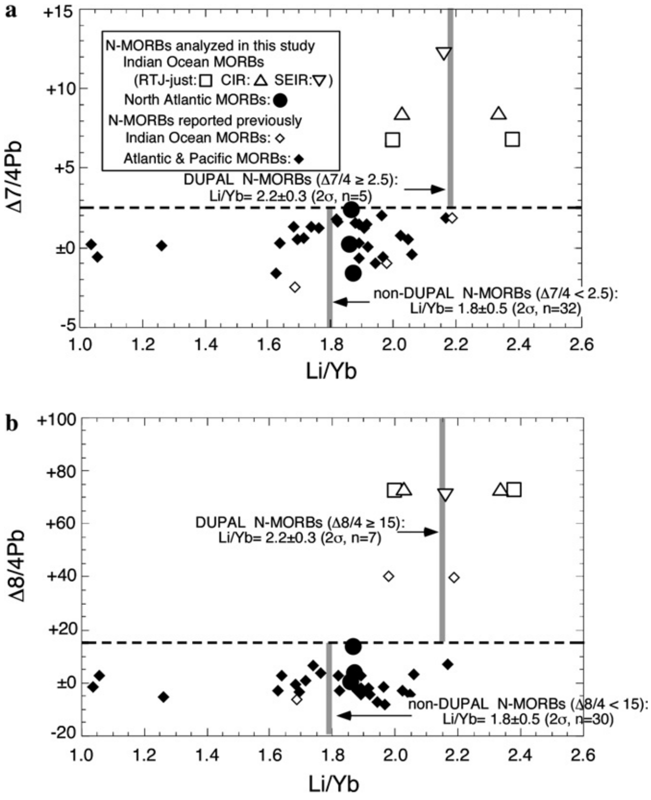

Fig. 3. Li/Yb weight ratios as a function of Δ7/4Pb (a) and Δ8/4Pb (b) of N-MORBs [$SiO_2 = 45–52$ wt%; $(La/Sm)_n < 1$]. The Pb isotopic composition of North Atlantic MORB sample CH98-DR11 has been previously reported (Hamelin et al., 1984). Because the Pb isotopic compositions of other MORB samples have not been documented, we estimated the Δ7/4Pb and Δ8/4Pb values of the sampling area from available N-MORB data (Appendix 4). These diagrams also show data from other N-MORBs whose SiO_2, Li, Yb, La, and Sm contents, and Pb isotopic compositions are available (Appendix 5).

in Indian Ocean MORBs and the E-MORB-type enriched mantle source have quite different $C/^3He$ values, which are, respectively, low ($<1 \times 10^9$) and high ($\sim 4 \times 10^9$). Consequently, subducted sedimentary carbon with high $C/^3He$ can be definitively rejected as the source of the Indian Ocean DUPAL signature.

5.4.2. Lower continental crust (LCC)

Hanan et al. (2004) reported that Indian Ocean DUPAL MORBs showing high Δ8/4Pb values have positive ΔεHf values (+8 to +1), which are significantly higher than those of non-DUPAL MORBs (+1 to −5). The ΔεHf value is defined as the vertical deviation from the εNd–εHf mantle array. The anomalously high ΔεHf values of the Indian Ocean DUPAL MORBs require a time-integrated Lu/Hf source composition substantially different from that of all other known oceanic basalt mantle sources, including those of both MORB and OIB. Based on these Hf isotopic results, Hanan et al. (2004) argued that a LCC possibly caused the DUPAL anomaly in Indian Ocean MORBs. Furthermore, Escrig et al. (2004) demonstrated that significant amounts of LCC melt are required to produce the Os–Pb–Sr–Nd isotopic composition of Indian Ocean DUPAL-type MORBs.

The δ^7Li and Yb/Li values of MORBs analyzed in this study are shown in Fig. 6 together with DM and LCC end-member values (Rudnick and Gao, 2003; Teng et al., 2004). The δ^7Li value of the DM end-member was estimated as +3.1‰ from the average of the N-Atlantic N-MORB data obtained in our study. The Yb/Li value of the DM was estimated to be 0.56 (Li/Yb = 1.8) from the average of the non-DUPAL N-MORBs with Δ8/4Pb values lower than 15 (Fig. 3b). The δ^7Li and Yb/Li values of LCC have been estimated to be +1‰ and 0.12 (Li/Yb = 8.7), respectively, from high-grade metamorphic terrane and granulite-facies xenolith data (Rudnick and Gao, 2003; Teng et al., 2004). Using these end-member values, the δ^7Li and Yb/Li values of the RTJ N-MORBs can be explained by binary mixing of DM and LCC components (Fig. 6). In this case, about 20% of Li in RTJ MORBs can be attributed to recycled LCC. Our estimation using Li data agrees with a previous estimation using the radiogenic isotope compositions of Os, Pb, Sr, and Nd (Escrig et al., 2004): Escrig et al. (2004) proposed that about 10% of the melt should be derived from LCC in order to produce the Os–Pb–Sr–Nd isotopic compositions of RTJ MORBs. During the melting process, mafic rocks are expected to be more fertile than the peridotitic mantle, and thus to melt to a higher degree, so that their contribution in the liquid phase is increased by a factor of three to four compared with the pristine solid mafic–ultramafic proportions (Hirschmann and Stolper, 1996). Taking this effect into consideration, Escrig et al. (2004) further pointed out that the DUPAL signature of RTJ MORBs requires less than 4% of LCC to be added to its source. Thus, the Li isotope data support the previous proposal that significant amounts of recycled LCC are probably the cause of the Indian Ocean DUPAL signature.

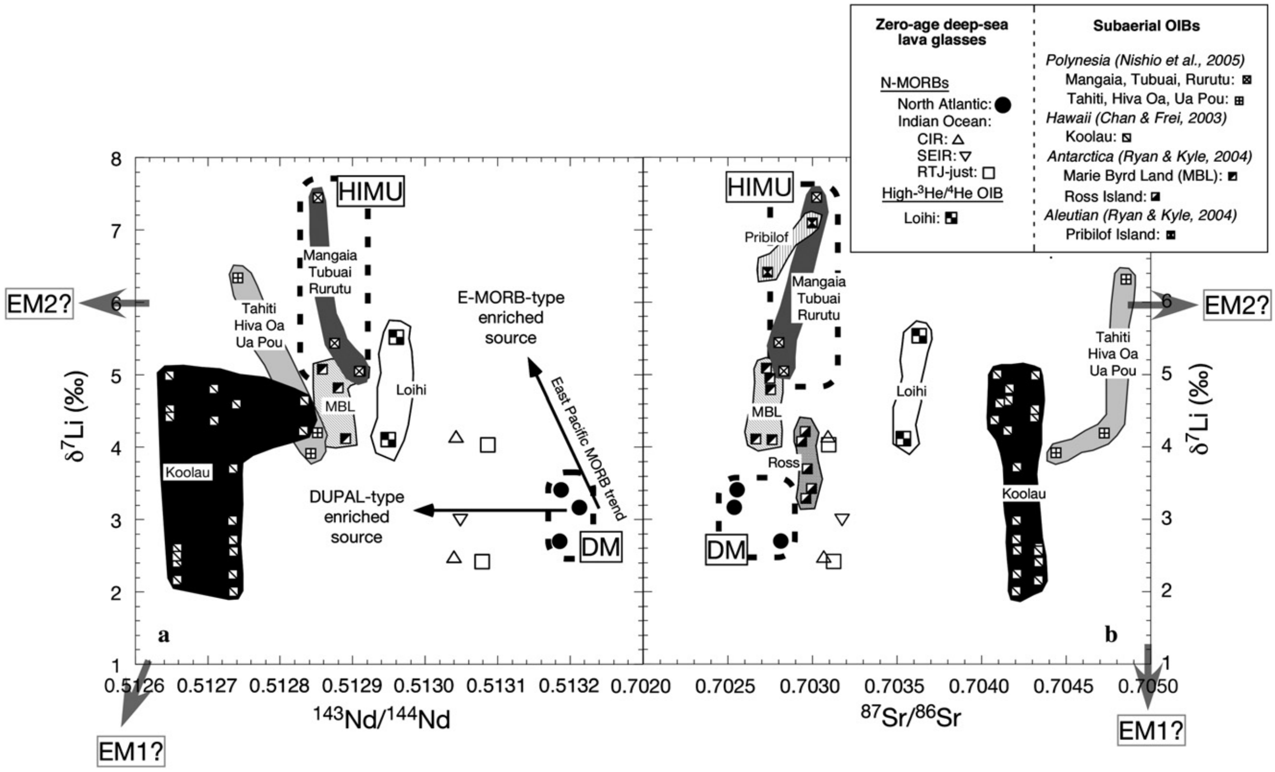

Fig. 4. δ^7Li values as a function of the ^{143}Nd/^{144}Nd (a) and ^{87}Sr/^{86}Sr (b) of MORBs and OIBs. MORB and Loihi OIB glass data were determined in this study. Subaerial OIB data are from the following papers: Polynesia [Mangaia, Tubuai, Rurutu, Tahiti, Hiva Oa, and Ua Pou] (Nishio et al., 2005); Hawaii [Koolau] (Chan and Frey, 2003); Antarctica [Marie Byrd Land and Ross Island] and the Aleutian Islands [Pribilof Island] (Ryan and Kyle, 2004). The Nd and Sr isotopic compositions of the mantle reservoirs (DM, HIMU, EM1, and EM2) are from Zindler and Hart (1986). The δ^7Li value of the DM reservoir was estimated from the N-Atlantic N-MORB data determined in this study. The δ^7Li value of the HIMU reservoir was estimated from HIMU OIB data (Nishio et al., 2005). The δ^7Li values of the EM1 and EM2 reservoirs were estimated from mantle-derived xenolith data (Nishio et al., 2004).

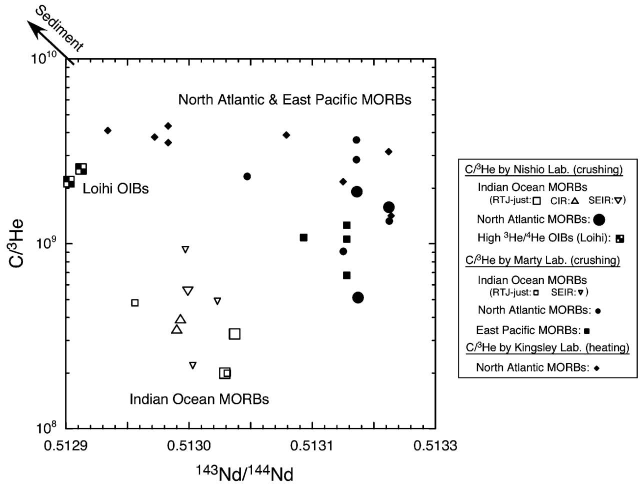

Fig. 5. Correlation of ^{143}Nd/^{144}Nd ratios and C/^{3}He mole ratios of MORB glasses from N-Atlantic, E-Pacific, and Indian Ocean. The C/^{3}He values in this figure were determined by three separate laboratories: Kingsley Lab (Kingsley and Schilling, 1995), Marty Lab. (Marty and Tolstikhin, 1998; Marty and Zimmermann, 1999), and Nishio Lab. (this study and 1999). The C/^{3}He values of Kingsley Lab were estimated from vesicle-C/^{3}He values determined using the stepwise heating technique, while the C/^{3}He values of the Marty and Nishio Labs were estimated from vesicle-CO$_2$/^{3}He values determined using the crushing technique. The data shown are from the relatively less degassed samples (^{4}He/^{40}Ar* ⩽30) only, except for the data from the Kingsley Lab, for which ^{4}He/^{40}Ar* is unknown (Kingsley and Schilling, 1995). The ^{143}Nd/^{144}Nd data sources are listed in Appendix 6.

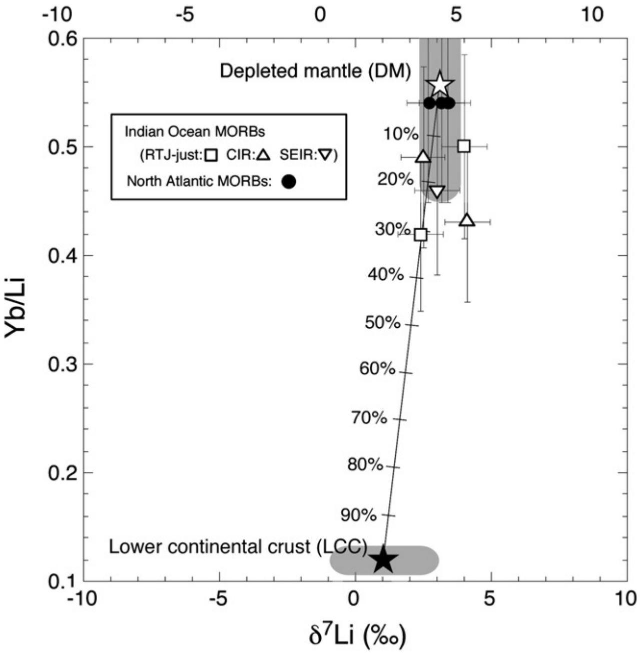

Fig. 6. Correlation of δ^7Li values and Yb/Li weight ratios of MORB glasses. Solid line indicates a binary mixing trend between depleted mantle (DM) and lower continental crust (LCC). The δ^7Li and Li/Yb values of the DM and LCC sources are explained in the text. Errors shown are listed in Table 1.

6. Conclusions

No systematic Li isotopic difference was observed between the RTJ DUPAL N-MORBs (+3.2 ± 1.6‰, 2SD) and the N-Atlantic non-DUPAL N-MORBs (+3.1 ± 0.7‰, 2SD). Thus, the source of the DUPAL signature in Indian Ocean MORBs and the source of E-MORB-type enriched mantle have quite different δ^7Li values, which are +3‰ and >+5‰, respectively (Elliott et al., 2003). The ^{143}Nd/^{144}Nd values of both sources are lower than those of the North Atlantic N-MORBs. The δ^7Li values of most OIBs related to HIMU and/or EM2 sources are also higher than that of DM (+3‰) (Chan and Frey, 2003; Ryan and Kyle, 2004; Nishio et al., 2005). In contrast, the δ^7Li values of several Koolau OIBs are significantly lower than those of other OIBs with low ^{143}Nd/^{144}Nd signature (Chan and Frey, 2003). Thus, we inferred that the relatively low δ^7Li values of the Indian Ocean DUPAL N-MORBs and several Koolau OIBs can be attributed to an EM1 reservoir.

Based on the Hf isotopic results, Hanan et al. (2004) argued that LCC was a possible cause of the DUPAL anomaly in Indian Ocean MORBs. Our Li isotope results can be explained by a model in which significant amounts of recycled LCC produce the DUPAL isotopic signatures of the Indian Ocean MORB source.

Acknowledgments

This manuscript benefited from thoughtful and constructive reviews and improvements in English expression by Marissa Tejada. We are grateful to Harue Masuda (TAG samples) and Hajime Hiyagon (CH31–CH98 samples) for providing the N-Atlantic MORB samples, and Toshitaka Gamo for providing the Loihi samples. We also thank W. Soh and staff of the Kochi Core Center who have made every effort to provide an excellent research environment for Y. Nishio. Special thanks to K. Sato, H. Yamaguchi, M. Sakaguchi, and N. Takahata for their help with analyses of major and volatile elements, respectively. Comments from T. Matsumoto, J. Yamamoto, M. Handler, H. Amakawa, T. Hanyu, H. Kumagai, T. Ishikawa, and K. Suzuki are also gratefully acknowledged. We thank Y. Tatsumi and S. Nakada for supporting this work. The "Petrological Database of the Ocean Floor (PETDB, http://www.petdb.org/)" was used for obtaining previously reported abyssal glass data. This study was supported by the following grants: a Grant-in-Aid for Scientific Research to Y. Nishio (No. 16740309) and H. Kumagai (No. 14540457) from the Ministry of Education, Culture, Sports, Science and Technology of Japan. Reviews by Bernard Marty, Jon Snow, Paul Tomascak, and an anonymous referee helped to clarify the presentation and are greatly appreciated.

Associate editor: Bernard Marty

Appendix 1

Trace elemental abundances of studied marginal glasses of pillow lavas from the mid-oceanic ridge and the southern rift zone of Loihi Seamount, Hawaii

Sample	Indian Ridges (Triple Junction area)					North Atlantic Ridge			Seamount (Hawaii)		Reference Data	
	KH93-3-DR3-A1	KH93-3-DR1-F1	KH93-3-DR9-G1	KH93-3-DR25-A1	KH93-3-DR6-A1	224-R-01	CH98-DR11	CH31-DR11	KH85-4-DE54-025	KH85-4-DE55-1	JB-1a	(2RSD)[a]
Li abundance (μg g^{-1}) *determined by MC-ICP-MS after Li-purification*												
Li	6.76	5.59	7.63	6.24	5.60	6.14	6.73	6.32	4.65	5.65	10.6	(12%)
Other trace element abundances (μg g^{-1}) *determined by quadruple ICP-MS without purification*												
Rb	0.45	1.63	0.87	0.48	0.89	0.88	0.70	2.58	10.0	9.27	10.4	(5%)
Sr	112	140	96.6	97.8	120	111	92.8	96.4	324	373	241	(9%)
Y	25.7	24.8	33.9	25.6	23.4	29.9	31.5	29.4	17.9	20.4	24.7	(7%)
Ba	7.46	17.7	11.4	6.12	13.3	9.09	11.2	31.3	133	139	274	(5%)
La	2.54	3.69	3.49	2.45	2.59	3.40	2.84	4.44	15.1	14.6	4.90	(7%)
Ce	8.43	10.7	11.4	7.96	8.21	10.3	9.17	11.6	30.3	34.2	12.5	(7%)
Pr	1.50	1.79	1.98	1.44	1.40	1.82	1.63	1.90	4.77	4.60	2.01	(9%)
Nd	8.30	8.85	10.8	7.73	7.77	10.0	9.28	9.78	18.8	22.2	10.1	(7%)
Sm	3.08	2.85	3.63	2.83	2.72	3.57	3.44	3.30	5.23	5.61	3.17	(10%)
Eu	1.16	1.16	1.40	1.10	1.05	1.31	1.34	1.28	1.79	1.97	1.11	(13%)
Gd	4.09	3.79	5.31	3.70	3.29	4.72	4.65	4.24	4.79	5.78	3.74	(6%)
Tb	0.75	0.73	0.96	0.73	0.65	0.89	0.95	0.85	0.88	0.90	0.72	(8%)
Dy	5.04	4.70	6.20	4.72	4.40	5.68	6.23	5.58	4.35	4.85	4.44	(7%)
Ho	1.09	0.97	1.37	1.00	0.92	1.24	1.36	1.18	0.79	0.86	0.99	(6%)
Er	3.20	2.86	4.05	3.15	2.52	3.69	3.93	3.42	1.82	2.19	2.83	(8%)
Tm	0.45	0.44	0.62	0.44	0.41	0.53	0.59	0.51	0.28	0.29	0.43	(11%)
Yb	2.89	2.76	3.82	2.63	2.59	3.29	3.61	3.40	1.57	1.79	2.73	(12%)
Lu	0.39	0.41	0.51	0.40	0.37	0.49	0.57	0.52	0.25	0.27	0.43	(11%)

[a] Relative standard deviation (2σ) of repeated measurements of JA-1 (Li, $n = 5$; other elements, $n = 7$).

Appendix 2

Volatile data (C–N–He–Ar) of vesicle-gas and the chemical compositions of marginal glasses of pillow lavas from the North Atlantic TAG and the Loihi

Sample	224-R-01	KH85-4-DE54-025	KH85-4-DE55-1
Volatile data			
Crushing 1 (for He isotopic data)			
Sample weight (g)	1.24	0.35	2.42
Isotopic ratios			
$^{3}He/^{4}He$ (R/R_A)[a]	8.46	30.4	24.6
Concentrations			
^{4}He ($\times 10^{-10}$ mol/g)	6.3	0.18	0.96
Crushing 2 (for C–N–Ar data)			
Sample weight (g)	2.76	0.82	1.66
Isotopic ratios			
$^{40}Ar/^{36}Ar$	6760	490	669
$\delta^{13}C$ (‰) of CO_2	−2.77	−1.36	−1.90
$\delta^{15}N$ (‰) of N_2	−3.2	+0.5	+0.4
Concentrations			
CO_2 ($\times 10^{-6}$ mol/g)	1.88	5.73	8.09
N_2 ($\times 10^{-9}$ mol/g)	2.8	8.6	11.1
^{4}He ($\times 10^{-10}$ mol/g)	3.1	0.53	1.06
^{40}Ar ($\times 10^{-11}$ mol/g)	2.5	10.7	13.6
Major elemental abundances[b]			
SiO_2	49.6	46.3	46.9
Al_2O_3	14.9	13.4	12.7
TiO_2	1.63	3.41	2.96
Fe_2O_3	11.0	11.6	13.2
MnO	0.18	0.19	0.18
MgO	8.77	6.39	7.86
CaO	11.1	11.7	12.2
Na_2O	2.82	2.29	2.56
K_2O	0.08	0.78	0.57
P_2O_5	0.16	nd	0.30
Total	100.6	95.97	99.50

[a] Sample $^{3}He/^{4}He$ ratios are normalized to the atmospheric $^{3}He/^{4}He$ ratio, $R_A = 1.4 \times 10^{-6}$. The $^{3}He/^{4}He$ ratios listed in this table were measured by a noble gas mass spectrometer (6-60-SGA, Nuclide CO.) without separating He from Ne. It has, however, been reported that there is a systematic difference of 8.9% in the $^{3}He/^{4}He$ ratios between Nuclide and VG5400 instruments which is possibly caused by Ne interference on He isotope measurements (Sano et al., 1998). Then, the $^{3}He/^{4}He$ ratios obtained by 6-60-SGA are corrected for the difference of analytical system (Nishio et al., 1999).

[b] 224-R-001 and KH85-4-DE55-1 data were determined by XRF. KH85-4-DE54-025 data were determined by EPMA. The listed EPMA data is the average of 10 spot data. (nd, data were not determined).

Appendix 3

End-member values on the binary mixing calculation shown in Fig. 1c

	Deep seawater (Indian Ocean)	MORB (North Atlantic)
$^{87}Sr/^{86}Sr$	0.709[a]	0.7025[d]
Sr (mol g^{-1})	9.1×10^{-8} [b]	1.2×10^{-6} [e]
$^{143}Nd/^{144}Nd$	0.51223[c]	0.51321[e]
Nd (mol g^{-1})	2.5×10^{-14} [c]	6.3×10^{-8} [f]

[a] Data from Palmer and Edmond (1989).

[b] Data from Bruland and Lohan (2003).

[c] Data from Goldstein and Hemming (2003).

[d] The lowest $^{87}Sr/^{86}Sr$ of North Atlantic MORBs analyzed in this study.

[e] Average values of North Atlantic MORBs analyzed in this study.

[f] The highest $^{143}Nd/^{144}Nd$ of North Atlantic MORBs analyzed in this study.

Appendix 4

Sample ID (this study)	$^{206}Pb/^{204}Pb$	$^{207}Pb/^{204}Pb$	$^{208}Pb/^{204}Pb$	Δ7/4Pb	Δ8/4Pb	References (sample ID)
Sample whose Pb isotopes have already been reported						
CH98-DR11	18.084	15.476	37.627	2.5	13.6	Hamelin et al. (1984) (CHR0098-011)
Samples whose Pb isotopes have never been reported (Pb isotopes were estimated from reported adjacent MORB data)						
KH93-3-DR3-A1	17.316	15.452	37.290	8.4	72.8	Michard et al. (1986) (DUF0023-003-001)
KH93-3-DR1-F1	17.316	15.452	37.290	8.4	72.8	Michard et al. (1986) (DUF0023-003-001)
KH93-3-DR9-G1	17.488	15.455	37.500	6.8	73.0	Michard et al. (1986) (CHRRODR-3-003-001)
KH93-3-DR25-A1	17.488	15.455	37.500	6.8	73.0	Michard et al. (1986) (CHRRODR-3-003-001)
KH93-3-DR6-A1	17.661	15.528	37.697	12.3	71.8	Price et al. (1986) (AII0093-6-013-001)
224-R-01	18.123	15.440	37.579	−1.6	4.1	Hamelin et al. (1984) (CHR0098-015)
CH31-DR11	18.790	15.530	38.350	0.2	0.6	Dupre et al. (1981) (ARP1974-007-005C)

Appendix 5

Sample ID	SiO_2 (wt%)	MgO (wt%)	$^{87}Sr/^{86}Sr$	$^{143}Nd/^{144}Nd$	$^{206}Pb/^{204}Pb$	$^{207}Pb/^{204}Pb$	$^{208}Pb/^{204}Pb$	Δ7/4Pb	Δ8/4Pb	$(La/Sm)_n$	$(La/Yb)_n$	$(Sm/Yb)_n$	Li/Y	Li/Yb	References
North Atlantic MORB															
ALV0534-002-001	50.3	9.91	0.70288	0.513079	18.899	15.545	38.435	0.53	−4.09				0.190		Bryan and Moore (1977), Bryan et al. (1979), Ito et al. (1987)
East Pacific MORBs															
108DR1	50.3	7.80	0.70291	0.513120	18.405	15.492	37.885	0.59	0.64	0.80	0.90	1.13		1.71	Prinzhofer et al. (1989)
108DR4	51.5	7.79	0.70269	0.513159	18.297	15.477	37.774	0.26	2.59	0.70	0.82	1.17		1.64	Prinzhofer et al. (1989)
CYA1982-001-004	50.6	8.49	0.70261	0.513098	18.427	15.502	37.900	1.35	−0.52	0.56	0.61	1.08		1.68	Prinzhofer et al. (1989)
CYA1982-006-001	49.6	8.28	0.70288	0.513118	18.271	15.484	37.753	1.24	3.64	0.38	0.41	1.09	0.165	1.76	Prinzhofer et al. (1989); Hekinian et al., 1989
CYA1982-018-001	49.8	7.53	0.70260	0.513111	18.390	15.487	37.844	0.25	−1.65	0.90	1.11	1.23		1.04	Prinzhofer et al. (1989)
CYA1982-020-002	49.8	8.11	0.70271	0.513120	18.385	15.485	37.801	0.11	−5.35	0.53	0.54	1.01		1.26	Prinzhofer et al., 1989
CYA1982-021-004	50.1	8.60	0.70253	0.513130	18.200	15.460	37.663	−0.39	3.22	0.80	1.15	1.44	0.174	2.06	Prinzhofer et al. (1989), Hekinian et al. (1989)
CYA1982-027-001	50.8	7.64	0.70256	0.513103	18.327	15.491	37.850	1.34	6.57	0.74	1.02	1.37	0.155	1.74	Prinzhofer et al. (1989); Hekinian et al. (1989)
CYA1982-027-002	49.8	7.96	0.70260	0.513137	18.380	15.502	37.918	1.86	6.96	0.75	1.11	1.48	0.186	2.17	Prinzhofer et al. (1989); Hekinian et al. (1989)
CYA1982-027-005	49.8	8.56	0.70274	0.513139	18.294	15.468	37.774	−0.61	2.96	0.93	1.22	1.31		1.06	Prinzhofer et al., 1989
MELPHNX-2-044-002	51.4	5.73	0.70268	0.513157	18.315	15.484	37.738	0.77	−3.18	0.65	0.79	1.21	0.208	2.02	Regelous et al. (1999)
MELPHNX-2-045-001	51.6	3.27	0.70254	0.513159	18.299	15.480	37.718	0.54	−3.25	0.74	0.93	1.25	0.177	1.70	Regelous et al. (1999)
MELPHNX-2-047-003	51.4	5.28	0.70256	0.513152	18.337	15.494	37.769	1.53	−2.74	0.77	0.94	1.23	0.195	1.88	Regelous et al. (1999)
MELPHNX-2-051-005	51.6	5.66	0.70252	0.513167	18.311	15.479	37.723	0.31	−4.20	0.67	0.76	1.14	0.201	1.89	Regelous et al. (1999)
MELPHNX-2-054-003	51.0	6.99	0.70247	0.513180	18.248	15.463	37.607	−0.61	−8.18	0.58	0.66	1.14	0.207	1.97	Regelous et al. (1999)
MELPHNX-2-055-003	50.8	6.31	0.70253	0.513153	18.321	15.467	37.706	−1.00	−7.11	0.64	0.74	1.15	0.202	1.94	Regelous et al. (1999)
MELPHNX-2-056-002	50.8	6.67	0.70255	0.513159	18.322	15.492	37.758	1.49	−2.03	0.66	0.77	1.17	0.200	1.92	Regelous et al. (1999)
MELPHNX-2-060-002	50.3	4.93	0.70253	0.513157	18.296	15.475	37.703	0.07	−4.39	0.68	0.82	1.20	0.198	1.92	Regelous et al. (1999)
MELPHNX-2-062-001	50.5	6.10	0.70254	0.513150	18.321	15.497	37.762	2.00	−1.51	0.69	0.83	1.20	0.204	1.96	Regelous et al. (1999)
MELPHNX-2-063-001	50.7	5.62	0.70255		18.347	15.492	37.779	1.22	−2.95	0.68	0.80	1.17	0.200	1.91	Regelous et al. (1999)
MELPHNX-2-068-001	50.4	6.87	0.70259	0.513167	18.307	15.492	37.732	1.65	−2.82	0.72	0.87	1.21	0.190	1.82	Regelous et al. (1999)
MELPHNX-2-069-002	50.6	6.73	0.70255	0.513156	18.338	15.484	37.754	0.52	−4.36	0.69	0.80	1.16	0.213	2.05	Regelous et al. (1999)
MELPHNX-2-077-006	51.5	5.84	0.70251	0.513173	18.305	15.490	37.737	1.47	−2.07	0.65	0.76	1.17	0.196	1.89	Regelous et al. (1999)
NHOCHEP-003-003	49.5	7.50	0.70256	0.513140	18.295	15.468	37.774	−0.62	2.83			1.12	0.187	1.89	Ryan and Langmuir (1987), Castillo et al. (2000)
NHOCHEP-004-001	50.0	7.04	0.70261	0.513078	18.487	15.513	38.007	1.80	2.92			1.32	0.173	1.82	Ryan and Langmuir (1987), Castillo et al. (2000)
NHOCHEP-026-001	49.7	6.40	0.70255	0.513141	18.368	15.466	37.803	−1.61	−3.09			1.27	0.170	1.63	Ryan and Langmuir (1987), Castillo et al. (2000)
Indian Ocean MORBs															
MOA8801-016-012	50.1	7.79	0.70258	0.513064	18.798	15.504	38.291	−2.47	−6.28	0.94	1.29	1.36	0.176	1.69	Pyle et al. (1992), Danyushevsky et al. (2000)
VEM0033-2-007-003	51.2	7.33	0.70290	0.513037	18.057	15.439	37.858	−0.94	40.01	1.00	1.34	1.34	0.200	1.98	Ryan and Langmuir (1987), Klein et al. (1988), Klein et al. (1991)
VEM0033-2-007-007	49.9	9.11	0.70300	0.513007	18.008	15.462	37.794	1.89	39.53	0.79	1.00	1.27	0.207	2.19	Ryan and Langmuir (1987), Klein et al. (1988), Klein et al. (1991)

Appendix 6

Sample ID (C–He–Ar data)	^{4}He/^{40}Ar*	C/^{3}He ($\times 10^{9}$)	References of C–He–Ar data	^{143}Nd/^{144}Nd	References of Nd data (sample ID)
Vesicle-C/^{3}He measured by Marty Lab. (crushing)					
North Atlantic MORBs					
2PD-43	1.2	2.3	Marty and Tolstikhin (1998)	0.513097	Dosso et al. (1991) (ABP1985-043-003)
CH98-11	6.2	1.3	Marty and Tolstikhin (1998)	0.513212	This study (CH98-DR11)
CH98-DR15	4.5	0.91	Marty and Tolstikhin (1998)	0.513175	Chauvel and Blichert-Toft (2001) (CHR0098-015)
CH31-DR11	13	3.7	Marty and Tolstikhin (1998)	0.513186	This study (CH31-DR11)
CH31-DR11 No. 4	19	2.9	Marty and Tolstikhin (1998)	0.513186	This study (CH31-DR11)
East Pacific MORBs					
CL-DR01-5V	15	0.68	Marty and Tolstikhin (1998)	0.513178	Chaussidon et al. (1991) (CHRCLIP-001-005V)
CL-DR01-5V-B	17	1.1	Marty and Tolstikhin (1998)	0.513178	Chaussidon et al. (1991) (CHRCLIP-001-005V)
CL-DR01	21	1.3	Marty and Zimmermann (1999)	0.513178	Chaussidon et al. (1991) (CHRCLIP-001-005V)
NAUDUR-DR21-4	19	1.1	Marty and Zimmermann (1999)	0.513143	Schiano et al. (1997) (NADNAUD-021-004)
Indian Ocean MORBs (*Rodrigues Triple Junction*)					
JC0300703D1	7.2	0.48	Marty and Zimmermann (1999)	0.513006	Salters (1996) (JC0300703D1)
MD 23 SITE 4	2.2	0.20	Marty and Zimmermann (1999)	0.513081	Salters (1996) (DUF0023-004-004)
MD23 SITE2	5.7	0.93	Marty and Zimmermann (1999)	0.513047	Michard et al. (1986) (DUF0023-002-001)
MD37 05/03 D1	6.0	0.22	Marty and Zimmermann (1999)	0.513053	Hamelin et al. (1986) (DUF0037-003-001)
Indian Ocean MORBs (*Southeast Indian Ridge*)					
HY09-07H	16	0.49	Marty and Zimmermann (1999)	0.513073	Dosso et al. (1988) (CHRHYAM-009-007)
Vesicle-C/^{3} He measured by Kingsley Lab. (heating)					
North Atlantic MORBs					
TR123-5D		3.2	Kingsley and Schilling (1995)	0.513212	Kingsley and Schilling (1995)
TR123-1D		3.9	Kingsley and Schilling (1995)	0.513129	Kingsley and Schilling (1995)
TR89-30D		4.3	Kingsley and Schilling (1995)	0.513033	Kingsley and Schilling (1995)
TR154-17D		3.5	Kingsley and Schilling (1995)	0.513033	Kingsley and Schilling (1995)
TR154-16D		3.8	Kingsley and Schilling (1995)	0.513022	Kingsley and Schilling (1995)
TR154-14D		4.1	Kingsley and Schilling (1995)	0.512984	Kingsley and Schilling (1995)
TR138-7D		1.4	Kingsley and Schilling (1995)	0.513214	Kingsley and Schilling (1995)
EN025-4D		2.2	Kingsley and Schilling (1995)	0.513175	Kingsley and Schilling (1995)

References

Agranier, A., Blichert-Toft, J., Graham, D., Debaille, V., Schiano, P., Albarede, F., 2005. The spectra of isotopic heterogeneities along the mid-Atlantic Ridge. *Earth Planet. Sci. Lett.* **238**, 96–109.

Bougault, H., Hekinian, R., 1974. Rift valley in the atlantic ocean near 36°50′N: petrology and geochemistry of basaltic rocks. *Earth Planet. Sci. Lett.* **24**, 249–261.

Bougault, H., Treuil, M., 1980. Mid-Atlantic Ridge: zero-age geochemical variations between Azores and 22°N. *Nature* **286**, 209–212.

Brenan, J.M., Neroda, E., Lundstrom, C.C., Shaw, H.F., Ryerson, F.J., Phinney, D.L., 1998. Behaviour of boron, beryllium, and lithium during melting and crystallization: constraints from mineral-melt partitioning experiments. *Geochim. Cosmochim. Acta* **62**, 2129–2141.

Bruland, K.W., Lohan, M.C., 2003. Controls of Trace Metals in Seawater. In: Holland, H.D., Turekian, K.K. (Eds.), *Treatise on Geochemistry*, vol. 6.02. Elsevier Science Ltd, pp. 23–47.

Bryan, W.B., Moore, J.G., 1977. Compositional variations of young basalts in the Mid-Atlantic Ridge rift valley near Lat 36 degree 49°N. *USGS BULL* **88**, 556–570.

Bryan, W.B., Thompson, G., Michael, P.J., 1979. Compostional variation in a steady-state zoned magma chamber: Mid-Atlantic Ridge at 36 degree 50°N. *Tectonophysics* **55**, 63–85.

Burnard, P., Graham, D., Turner, G., 1997. Vesicle-specific noble gas analyses of "popping rock": implications for primordial noble gases in earth. *Science* **276**, 568–571.

Castillo, P.R., Klein, E.M., Bender, J.F., Langmuir, C.H., Shirey, S.B., Bariza, R., White, W.M., 2000. Petrology and Sr, Nd, and Pb isotope geochemistry of mid-ocean ridge basalt glasses from the 11°45′N to 15°00′N. *Geochem. Geophys. Geosyst.* **1**. doi:10.1029/1999GC000024.

Chan, L.-H., Kastner, M., 2000. Lithium isotopic compositions of pore fluids and sediments in the Costa Rica subduction zone: implications for fluid processes and sediment contribution to the arc volcanoes. *Earth Planet. Sci. Lett.* **183**, 275–290.

Chan, L.-H., Frey, F.A., 2003. Lithium isotope geochemistry of the Hawaiian plume: Results from the Hawaii Scientific Drilling Project and Koolau Volcano. *Geochem. Geophys. Geosyst.* **4**. doi:10.1029/2002GC000365.

Chan, L.-H., Edmond, J.M., Thompson, G., Gillis, K., 1992. Lithium isotopic composition of submarine basalts: implications for lithium cycle in the oceans. *Earth Planet. Sci. Lett.* **108**, 151–160.

Chan, L.-H., Leeman, W.P., You, C.-F., 1999. Lithium isotopic composition of Central American Volcanic Arc lavas: implications for modification of subarc mantle by slab-derived fluids. *Chem. Geol.* **160**, 255–280.

Chan, L.-H., Alt, J.C., Teagle, D.A.H., 2002. Lithium and lithium isotope profiles through the upper oceanic crust: a study of seawater-basalt exchange at ODP Sites 504B and 896A. *Earth Planet. Sci. Lett.* **201**, 187–201.

Chaussidon, M., Sheppard, S.M.F., Michard, A., 1991. Hydrogen, sulphur and neodymium isotope variation in the mantle beneath the EPR at 12 deg 50 min N. *J. Geochem. Soc.* **3**, 325–337.

Chauvel, C., Blichert-Toft, J., 2001. A hafnium isotope and trace element perspective on melting of the depleted mantle. *Earth Planet. Sci. Lett.* **190**, 137–151.

Danyushevsky, L.V., Eggins, S.M., Falloon, T.J., Christie, D.M., 2000. H2O abundance in depleted to moderately enriched mid-ocean ridge magmas; Part I: Incompatible behaviour, implications for mantle storage, and origin of regional variations. *J. Petrol.* **41**, 1329–1364.

Dosso, L., Bougault, H., Beuzart, P., Calvez, J.-Y., Joron, J.-L., 1988. The geochemical structure of the South-East Indian Ridge. *Earth Planet. Sci. Lett.* **88**, 47–59.

Dosso, L., Hanan, B.B., Bougault, H., Schilling, J.-G., Joron, J.-L., 1991. Sr–Nd–Pb geochemical morphology between 10° and 17°N on the Mid-Atlantic Ridge: A new MORB isotope signature. *Earth Planet. Sci. Lett.* **106**, 29–43.

Dupre, B., Lambret, B., Rousseau, D., Allegre, C.J., 1981. Limitations on the scale of mantle heterogeneities under oceanic ridges. *Nature* **294**, 552–554.

Elliott, T., Thomas, A., Jeffcoate, A., Niu, Y., 2003. Li isotope composition of the upper mantle. *EOS, Trans., Am. Geophys. Union* **84** (46), Fall Meet. Suppl., Abstract V51A-01.

Elliott, T., Jeffcoate, A., Bouman, C., 2004. The terrestrial Li isotope cycle: light-weight constraints on mantle convection. *Earth Planet. Sci. Lett.* **220**, 231–245.

Escrig, S., Capmas, F., Dupre, B., Allegre, C.J., 2004. Osmium isotopic constraints on the nature of the DUPAL anomaly from Indian mid-ocean-ridge basalts. *Nature* **431**, 59–63.

Fujioka, K., Gamo, T., Konoshita, M., 1995. Cruise report of the Fleet of JAMSTEC for Deep Sea Research No. 1: MODE'94 Shinkai 6500 Dives in TAG Hydrothermal Mound on the Mid-Atlantic Ridge, JAMSTEC, pp. 226.

Goldstein, S.L., Hemming, S.R., 2003. Long-lived Isotopic Tracers in Oceanography, Paleoceanography, and Ice-sheet Dynamics. In: Holland, H.D., Turekian, K.K. (Eds.), *Treatise on Geochemistry*, vol. 6.17. Elsevier Science Ltd., pp. 453–489.

Hamelin, B., Dupre, B., Allegre, C.J., 1984. Lead-strontium isotopic variations along the East Pacific Rise and the Mid-Atlantic Ridge: a comparative study. *Earth Planet. Sci. Lett.* **67**, 340–350.

Hamelin, B., Dupre, B., Allegre, C.J., 1986. Pb–Sr–Nd isotopic data of Indian Ocean ridges: new evidence of large-scale mapping of mantle heterogeneities. *Earth Planet. Sci. Lett.* **76**, 288–298.

Hanan, B.B., Blichert-Toft, J., Pyle, D.G., Christie, D.M., 2004. Contrasting origins of the upper mantle revealed by hafnium and lead isotopes from the Southeast Indian Ridge. *Nature* **432**, 91–94.

Hart, S.R., 1969. K, Rb, Cs contents and K/Rb, K/Cs ratios of fresh and altered submarine basalts. *Earth Planet. Sci. Lett.* **6**, 295–303.

Hart, S.R., 1984. A large-scale isotope anomaly in the Southern Hemisphere mantle. *Nature* **309**, 753–757.

Hekinian, R., Thompson, G., Bideau, R.D., 1989. Axial and off-axial heterogeneity of basaltic rocks from the east Pacific rise at 12 degree 35°N–12 degree 51°N. *J. Geophys. Res.* **94**, 17437–17463.

Hilton, D.R., Hammerschmidt, K., Loock, G., Friedrichsen, H., 1993. Helium and argon isotope systematics of the central Lau Basin and Valu Fa Ridge: Evidence of crust/mantle interactions in a back-arc basin. *Geochim. Cosmochim. Acta* **57**, 2819–2841.

Hirschmann, M.M., Stolper, E.M., 1996. A possible role for garnet pyroxenite in the origin of the "garnet signature" in MORB. *Contrib. Mineral. Petrol.* **124**, 185–208.

Hiyagon, H., Ozima, M., Marty, B., Zashu, S., Sakai, H., 1992. Noble gases in submarine glasses from mid-oceanic ridges and Loihi seamount: Constraints on the early history of the Earth. *Geochim. Cosmochim. Acta* **56**, 1301–1316.

Ito, E., White, W.M., Göpel, C., 1987. The O, Sr, Nd and Pb isotope geochemistry of MORB. *Chem. Geol.* **62**, 157–176.

Kingsley, R.H., Schilling, J.-G., 1995. Carbon in Mid-Atlantic Ridge basalt glasses from 28°N to 63°N: Evidence for a carbon-enriched Azores mantle plume. *Earth Planet. Sci. Lett.* **129**, 31–53.

Klein, E.M., Langmuir, C.H., Zindler, A., Staudigel, H., Hamelin, B., 1988. Isotope evidence of a mantle convection boundary at the Australian-Antarctic Discordance. *Nature* **333**, 623–629.

Klein, E.M., Langmuir, C.H., Staudigel, H., 1991. Geochemistry of basalts from the Southeast Indian Ridge, 115°E–138°E. *J. Geophys. Res.* **96**, 2089–2107.

Kumagai, H., Kaneoka, I., 2003. Relationship between submarine MORB glass textures and atmospheric component of MORBs. *Chem. Geol.* **200**, 1–24.

Kumagai, H., Kaneoka, I., 2005. Noble gas signatures around the Rodriguez Triple Junction in the Indian Ocean: Constraints on magma genesis in a ridge system. *Geochim. Cosmochim. Acta* **69**, 5567–5583.

Marty, B., Jambon, A., 1987. C/^{3}He in volatile fluxes from the solid Earth: implications for carbon geodynamics. *Earth Planet. Sci. Lett.* **83**, 16–26.

Marty, B., Ozima, M., 1986. Noble gas distribution in oceanic basalt glasses. *Geochim. Cosmochim. Acta* **50**, 1093–1097.

Marty, B., Tolstikhin, I.N., 1998. CO_2 fluxes from mid-ocean ridges, arcs and plumes. *Chem. Geol.* **145**, 233–248.

Marty, B., Zimmermann, L., 1999. Volatiles (He, C, N, Ar) in mid-ocean ridge basalts: assessment of shallow-level fractionation and characterization of source composition. *Geochim. Cosmochim. Acta* **63**, 3619–3633.

McDonough, W.F., Sun, S.-S., 1995. The composition of the Earth. *Chem. Geol.* **120**, 223–253.

Michard, A., Montigny, R., Schlich, R., 1986. Geochemistry of the mantle beneath the Rodriguez Triple Junction and the South-East Indian Ridge. *Earth Planet. Sci. Lett.* **78**, 104–114.

Moore, J.G., Clague, D.A., Normark, W.R., 1982. Diverse basalt types from Loihi seamount, Hawaii. *Geology* **10**, 88–92.

Moriguti, T., Nakamura, E., 1998. Across-arc variation of Li isotopes in lavas and implications for crust/mantle recycling at subduction zones. *Earth Planet. Sci. Lett.* **163**, 167–174.

Nishio, Y., Nakai, S., 2002. Accurate and precise lithium isotopic determinations of igneous rock samples using multi-collector inductively coupled plasma mass spectrometry. *Anal. Chim. Acta* **456**, 271–281.

Nishio, Y., Sasaki, S., Gamo, T., Hiyagon, H., Sano, Y., 1998. Carbon and helium isotope systematics of North Fiji Basin basalt glasses: carbon geochemical cycle in the subduction zone. *Earth Planet. Sci. Lett.* **154**, 127–138.

Nishio, Y., Ishii, T., Gamo, T., Sano, Y., 1999. Volatile element isotopic systematics of the Rodrigues Triple Junction Indian Ocean MORB: implications for mantle heterogeneity. *Earth Planet. Sci. Lett.* **170**, 241–253.

Nishio, Y., Nakai, S., Hirose, K., Ishii, T., Sano, Y., 2002. Li isotopic systematics of volcanic rocks in marginal basins (abstract). *Geochim. Cosmochim. Acta* **66**, A556.

Nishio, Y., Nakai, S., Yamamoto, J., Sumino, H., Matsumoto, T., Prikhod'ko, V.S., Arai, S., 2004. Lithium isotopic systematics of the mantle-derived ultramafic xenoliths: implications for EM1 origin. *Earth Planet. Sci. Lett.* **217**, 245–261.

Nishio, Y., Nakai, S., Kogiso, T., Barsczus, H.G., 2005. Lithium, strontium, and neodymium isotopic compositions of oceanic island basalts in the Polynesian region: constraints on a Polynesian HIMU origin. *Geochem. J.* **39**, 91–103.

Palmer, M.R., Edmond, J.M., 1989. The strontium isotope budget of the modern ocean. *Earth Planet. Sci. Lett.* **92**, 11–26.

Price, R.C., Kennedy, A.K., Riggs-Sneeringer, M., Frey, F.A., 1986. Geochemistry of basalts from the Indian Ocean triple junction: implications for the generation and evolution of Indian Ocean ridge basalts. *Earth Planet. Sci. Lett.* **78**, 379–396.

Prinzhofer, A., Lewin, E., Allegre, C.J., 1989. Stochastic melting of the marble cake mantle: evidence from local study of the East Pacific Rise at 12°50′N. *Earth Planet. Sci. Lett.* **92**, 189–206.

Pyle, D.G., Christie, D.M., Mahoney, J.J., 1992. Resolving an isotopic boundary within the Australian-Antarctic discordance. *Earth Planet. Sci. Lett.* **112**, 161–178.

Regelous, M., Niu, Y., Wendt, J.I., Batiza, R., Greig, A., Collerson, K.D., 1999. Variations in the geochemistry of magmatism on the East Pacific Rise at 10°30′N since 800 ka. *Earth Planet. Sci. Lett.* **168**, 45–63.

Rehkamper, M., Hofmann, A.W., 1997. Recycled ocean crust and sediment in Indian Ocean MORB. *Earth Planet. Sci. Lett.* **147**, 93–106.

Roden, M.F., Trull, T., Hart, S.R., Frey, F.A., 1994. New He, Nd, Pb, and Sr isotopic constraints on the constitution of the Hawaiian plume: Results from Koolau Volcano, Oahu, Hawaii, USA. *Geochim. Cosmochim. Acta* **58**, 1431–1440.

Rona, P.A., Klinkhammer, G., Nelsen, T.A., Trefry, J.H., Elderfield, H., 1986. Black smokers, massive sulfides, and vent biota at the Mid-Atlantic Ridge. *Nature* **321**, 33–37.

Rudnick, R.L., Gao, S., 2003. Composition of the Continental Crust. In: Holland, H.D., Turekian, K.K. (Eds.), *Treatise on Geochemistry*, vol. 3. Elsevier Science Ltd, pp. 1–64.

Ryan, J.G., Kyle, P.R., 2004. Lithium abundance and lithium isotope variations in mantle sources: insights from intraplate volcanic rocks from Ross Island and Marie Byrd Land (Antarctica) and other oceanic islands. *Chem. Geol.* **212**, 125–142.

Ryan, J.G., Langmuir, C.H., 1987. The systematics of lithium abundances in young volcanic rocks. *Geochim. Cosmochim. Acta* **51**, 1727–1741.

Salters, V.J.M., 1996. The generation of mid-ocean ridge basalts from the Hf and Nd isotope perspective. *Earth Planet. Sci. Lett.* **141**, 109–123.

Sano, Y., Marty, B., 1995. Origin of carbon in fumarolic gas from island arc. *Chem. Geol.* **119**, 265–274.

Sano, Y., Williams, S.N., 1996. Fluxes of mantle and subducted carbon along convergent plate boundaries. *Geophys. Res. Lett.* **20**, 2749–2752.

Sano, Y., Takahata, N., Nishio, Y., Marty, B., 1998. Nitrogen recycling in subduction zones. *Geophys. Res. Lett.* **25**, 2289–2292.

Schiano, P., Birck, J.-L., Allègre, C.J., 1997. Osmium–strontium–neodymium–lead isotopic covariations in mid-ocean ridge basalt glasses and the heterogeneity of the upper mantle. *Earth Planet. Sci. Lett.* **150**, 363–379.

Takahata, N., Nishio, Y., Yoshida, N., Sano, Y., 1998. Precise isotopic measurements of nitrogen at sub-nanomole level. *Anal. Sci.* **14**, 485–491.

Teng, F.-Z., McDonough, W.F., Rudnick, R.L., Gao, S., 2004. Lithium isotopic composition of the deep continental crust. *EOS, Trans., Am. Geophys. Union* **85** (47), Fall Meet. Suppl., Abstract V51C-0597.

Tomascak, P.B., Langmuir, C.H., 1999. Lithium isotope variability in MORB. *EOS, Trans., Am. Geophys. Union* **80**, Fall Meet. Suppl., Abstract V11E-10.

Tomascak, P.B., Tera, F., Helz, R.T., Walker, R.J., 1999. The absence of lithium isotope fractionation during basalt differentiation: new measurements by multicollector sector ICP-MS. *Geochim. Cosmochim. Acta* **63**, 907–910.

Valbracht, P.J., Staudacher, T., Malahoff, A., Allègre, C.J., 1997. Noble gas systematics of deep rift zone glasses from Loihi Seamount, Hawaii. *Earth Planet. Sci. Lett.* **150**, 399–411.

Verma, S.P., 1992. Seawater alteration effects on REE, K. Rb, Cs, Sr, U, Th, Pb and Sr–Nd–Pb isotope systematics of Mid-Ocean Ridge Basalt. *Geochem. J.* **26**, 159–177.

Yoshida, H., Takahashi, N., 1997. Chemical behavior of major and trace elements in the Horoman mantle diapir, Hidaka belt, Hokkaido, Japan. *J. Mineral. Petrol. Sci.* **92**, 391–409.

Zack, T., Tomascak, P.B., Rudnick, R.L., Dalpe, C., McDonough, W.F., 2003. Extremely light Li in orogenic eclogites: the role of isotope fractionation during dehydration in subducted oceanic crust. *Earth Planet. Sci. Lett.* **208**, 279–290.

Zindler, A., Hart, S., 1986. Chemical geodynamics. *Ann. Rev. Earth Planet. Sci.* **14**, 493–571.